Journal of Genetic Engineering and Biotechnology (2017) **15**, 505–513

HOSTED BY

ELSEVIER

Academy of Scientific Research & Technology and National Research Center, Egypt

Journal of Genetic Engineering and Biotechnology

www.elsevier.com/locate/jgeb

ORIGINAL ARTICLE

Characterization, synergistic antibacterial and free radical scavenging efficacy of silver nanoparticles synthesized using *Cassia roxburghii* leaf extract

Pooja Moteriya, Hemali Padalia, Sumitra Chanda *

Department of Biosciences (UGC-CAS), Saurashtra University, Rajkot 360 005, Gujarat, India

Received 18 January 2017; revised 11 May 2017; accepted 15 June 2017
Available online 13 July 2017

KEYWORDS

Cassia roxburghii;
Silver nanoparticles;
Characterization;
Synergistic antimicrobial activity;
Antioxidant activity

Abstract In this work, we report for the first time, synthesis of silver nanoparticles using *Cassia roxburghii* leaf extract and evaluate its synergistic antibacterial efficacy and antioxidant potential. The synergistic antimicrobial activity of silver nanoparticles with commercial antibiotics against Gram-positive, Gram-negative bacteria and fungi was evaluated. The antioxidant potential of synthesized silver nanoparticles was evaluated by FRAP and ABTS radical scavenging antioxidant assays. UV–Vis spectra peak at 473 and color change from colorless to brown color confirmed the formation of AgNPs. X-ray diffraction (XRD) and selected area electron diffraction (SAED) pattern confirmed the crystalline nature of synthesized nanoparticles. Transmission electron microscopy (TEM) analysis revealed the average size of particles to be 15–20 nm. Fourier transform infrared spectroscopy (FTIR) revealed the functional groups *C. roxburghii* leaf that was responsible for the reduction and capping process of nanoparticles. *C. roxburghii* leaf extract synthesized AgNPs showed good synergistic antimicrobial against Gram-negative bacteria even better than some of the antibiotics used as positive control; they also showed antioxidant potential. The results suggest that the synthesized nanoparticles can be used to treat multidrug resistant microorganisms and stress related diseases and disorders.

1. Introduction

The field of nanotechnology is the most active area of research in modern material science. Nanoparticles exhibit completely new or improved properties as compared to the larger particles of the bulk materials that they are composed of [1]. Nanoparticles are synthesized from various metals such as copper, zinc, titanium, magnesium, gold and silver. Their distinctive size-dependent properties make them superior and have numerous applications in various fields such as biotechnology, bioengineering, textile engineering, water treatment, metal-based consumer products and other areas such as electronic, magnetic, optoelectronics and information storage. However, silver nanoparticles (AgNPs) are of particular interest due to their specific properties and wide applications in different fields such as household appliances, catalysis, biosensing, imaging, drug

* Corresponding author.
E-mail address: svchanda@gmail.com (S. Chanda).
Peer review under responsibility of National Research Center, Egypt.

http://dx.doi.org/10.1016/j.jgeb.2017.06.010

delivery, nanodevice fabrication and in medicine [2]. Silver nanoparticles have also proved to have good antimicrobial efficacy. Green synthesis of silver nanoparticles and their antimicrobial activity has been reported by many researchers [3,4].

Nowadays mankind is faced with two problems viz. emergence of multidrug resistant bacteria and the infectious diseases caused by them which have become global health threat and diseases and disorders caused by free radicals. Antioxidants are compounds which are potential quenchers of free radicals and prevent them from attacking biological targets before they cause diseases i.e. they inhibit free radicals induced oxidative damage. Natural antioxidants are more popular than synthetic ones because they are easily available and nontoxic in nature.

Silver nanoparticles can be synthesized by physical, chemical or biological methods. However, the most popular method is biological synthesis because it is cost effective, environment friendly; easily scale-up for large scale synthesis and there is no need to use high pressure, energy, temperature or toxic chemicals [5]. Biological nanoparticles synthesis can be done by the use of microorganisms [6], enzymes [7] or plants (any part of the plant) such as *Bunium persicum* seed [8], *Dalbergia spinosa* leaf [9], *Piper longum* fruit [10] and *Cassia roxburghii* stem [11]. However use of plant extract mediated synthesis is more advantageous than other biological processes simply because the rate of reduction of metal ions is much faster, and stable nanoparticles are formed.

The *Cassia* genus (Family: Fabaceae) represents one of the largest and most diverse group of flowering plants, including herbs to trees. *Cassia* species have biological and medicinal activities such as immunomodulatory, antioxidant, antimicrobial and hypolipidemic [12,13]. Antimicrobial and antioxidant efficacy of AgNPs synthesized using *Cassia roxburghii* stem and synergistic antibacterial efficacy of AgNPs synthesized using *Cassia roxburghii* flower is already reported [11,14]. In the present work, silver nanoparticles were synthesized using aqueous leaf extract of *Cassia roxburghii* DC. Effect of boiling time for the preparation of plant extract and extract amount addition for the formation of silver nanoparticles was also standardized. The characterization was done by various spectral analyses such as UV–Vis spectra, FTIR, XRD, TEM and Zeta potential. The synthesized silver nanoparticles were evaluated for their synergistic antimicrobial activity with fifteen commercial antibiotics against four pathogenic bacteria and four fungi which included one clinical isolate. The antioxidant efficacy of synthesized silver nanoparticles was evaluated by ABTS and FRAP antioxidant assays.

2. Materials and methods

2.1. Chemicals and plant collection

The fresh leaves of *Cassia roxburghii* DC (CR) were collected from Saurashtra University campus, Rajkot, Gujarat, India. All the chemicals were obtained from Hi Media Laboratories and Sisco Research Laboratories Pvt. Limited, Mumbai, India. Milli Q water was used for all the experiments.

2.2. Preparation of the extract

Fresh leaves were thoroughly washed with tap water, followed by double distilled water and cut into small pieces. 5 g of cut leaves was boiled for 5 min in 100 ml ultra pure water and filtered through Whatman No. 1 filter paper. The filtered leaf extract was used for the synthesis of silver nanoparticles.

2.3. Synthesis of silver nanoparticles

Aqueous solution (1 mM) of silver nitrate ($AgNO_3$) was prepared and used for the synthesis of silver nanoparticles (AgNPs). 6 ml of aqueous leaf extract was added to 40 ml of 1 mM $AgNO_3$ solution for the reduction of Ag^+ ions. The synthesis of silver nanoparticles was carried out at room temperature (25 °C ± 2 °C) for 24 h in dark. The silver nanoparticles solution thus obtained was purified by repeated centrifugation at 10,000 rpm for 10 min followed by redispersion of the pellet of silver nanoparticles into acetone. After air drying of the purified silver particles, they were stored at 4 °C for further analysis.

2.4. Effect of boiling time

In order to standardize the effect of boiling time for the preparation of aqueous leaf extract of *C. roxburghii*, 5 g of cut leaves was taken in 100 ml ultra pure water and boiled for 5 min, 10 min and 15 min. and then filtered through Whatman No. 1 filter paper. The filtered *C. roxburghii* leaf extract was used for the synthesis of silver nanoparticles. The formation of AgNPs was monitored as a function of time of reaction on a spectrophotometer (Shimadzu UV-1601) by taking O.D. at 440 nm at an interval of 15 min.

2.5. Effect of extract amount

In order to standardize the effect of extract amount to be added to 1 mM $AgNO_3$ solution, different amount of extract (1.5 ml, 3.0 ml, 4.5 ml and 6.0 ml) was added to $AgNO_3$ solution. The formation of AgNPs was monitored as a function of time of reaction on a spectrophotometer (Shimadzu UV-1601) by taking O.D. at 440 nm at an interval of 15 min.

2.6. Characterization of the synthesized silver nanoparticles

The synthesis of silver nanoparticles was confirmed by UV–Vis absorption spectra. The reduction of the Ag^+ ions in solution was monitored by periodic sampling of reaction mixture, and the absorption maxima were scanned by UV–Vis spectrophotometer (Shimadzu UV-1601) in 400–700 nm range operated at an interval of 10 nm.

2.7. FTIR analysis

Possible functional groups involved in the synthesis and stabilization of silver nanoparticles were studied by FTIR spectroscopy. The FTIR spectra were recorded in the range of 400–4000 cm^{-1} Nicolet IS10 (Thermo Scientific, USA). The

various modes of vibrations were identified and assigned to determine the different functional groups present in the *C. roxburghii* leaf extract.

2.8. Zeta potential measurement

Zeta potential is an essential parameter for the characterization of stability in aqueous nano suspensions. The zeta potential measurement was performed using a Microtra (Zetatra Instruments).

2.9. XRD measurement

The structure and composition of synthesized AgNPs were analyzed by XRD. The formation of Ag nanoparticles was determined by an X'Pert Pro X-ray diffractometer (PAN analytical BV) operated at a voltage of 40 kV and a current of 30 mA with Cu Kα radiation in θ-2θ configurations. The crystallite domain size was calculated from the width of the XRD peaks, assuming that they are free from nonuniform strains, using the Scherrer formula. $D = 0.94\lambda/\beta \mathrm{Cos}\ \theta$ where D is the average crystallite domain size perpendicular to the reflecting planes, λ is the X-ray wavelength, β is the full width at half maximum (FWHM), and θ is the diffraction angle.

2.10. TEM analysis

TEM analysis was done to visualize the shape as well as to measure the diameter of the biologically synthesized silver nanoparticles. The sample was dispersed in double distilled

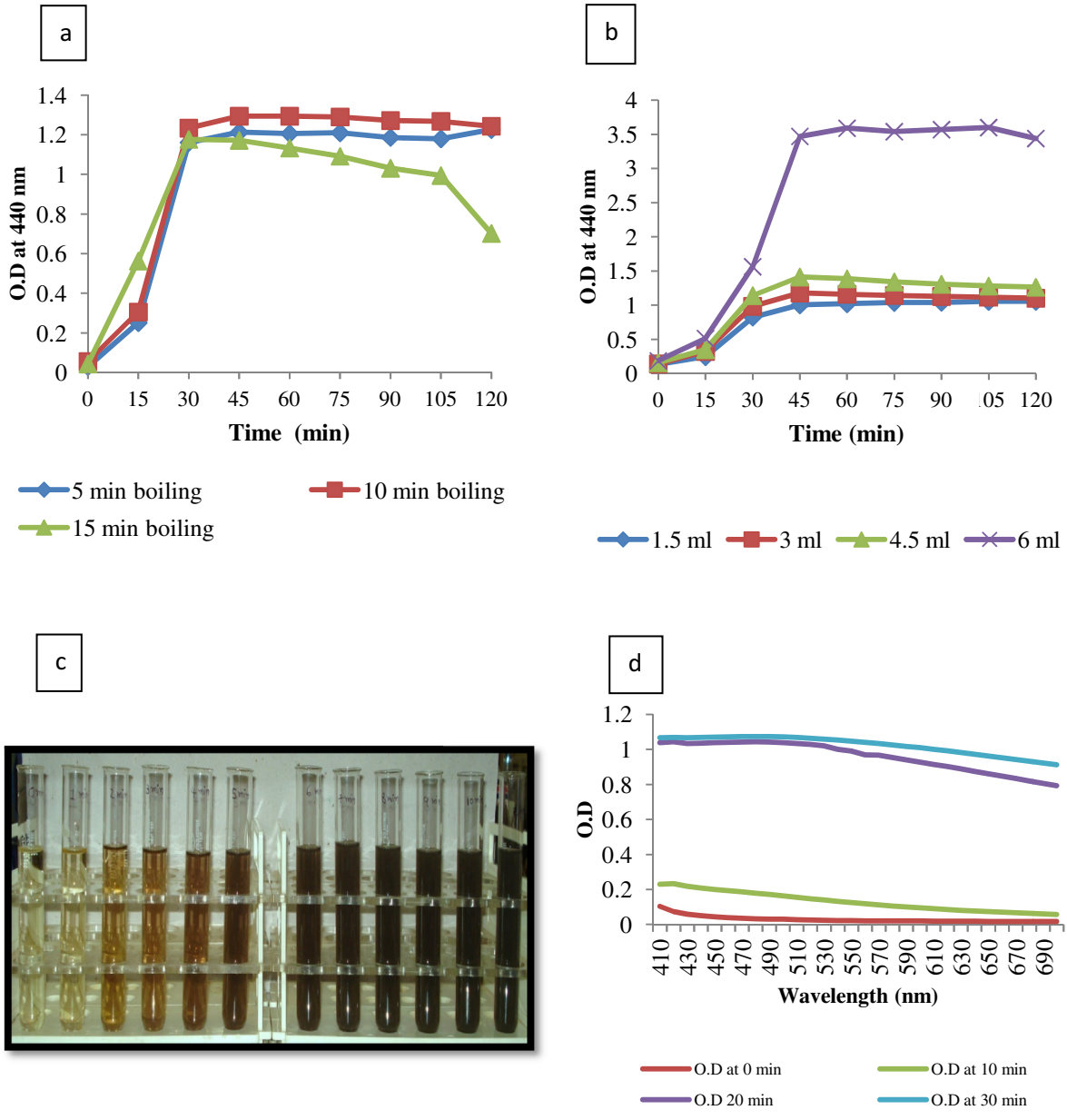

Fig. 1 (a) Effect of boiling time. (b) Effect of extract amount. (c) Color change in the reaction mixture within 10 min. (d) UV-Visible spectrum of biosynthesized AgNPs at different time interval.

water. A drop of thin dispersion was placed on a "staining mat". Carbon coated copper grid was inserted into the drop with the coated side upwards. After about ten minutes, the grid was removed and air-dried and then screened in JEOL JEM 2100 Transmission Electron Microscope.

2.11. Synergistic antimicrobial activity

The synergistic antimicrobial activity of 15 commercial antibiotics alone and antibiotics plus AgNPs was determined against 2 Gram-positive bacteria (*S. aureus* and *B. cereus*) and 2 Gram-negative bacteria (*E. coli* and *P. aeruginosa*) and 4 fungal (*C. albicans, C. glabrata, C. neoformans* and C 44, a clinical isolate) strains, by agar disk diffusion method [15]. 20 µl of 3 mg/ml AgNPs was loaded on to sterile disk. All experiments were performed in three replicates, and mean values are presented.

2.11.1. Assessment of increase in fold area

The increase in fold area was assessed by calculating the mean surface area of the inhibition zone of each antibiotic and antibiotic plus AgNPs. Increase in fold area was calculated as $(B^2 - A^2)/A^2$, where A and B are the inhibition zones for antibiotics and antibiotics + Ag-NPs, respectively.

2.12. Determination of antioxidant activities

The antioxidant activity of *C. roxburghii* leaf extract synthesized AgNPs was measured by two *in vitro* antioxidant assays viz. ABTS cation radical scavenging activity and FRAP activity. The details are as described earlier [16].

2.13. Qualitative phytochemical analysis

The crude powder of leaf was subjected to qualitative phytochemical analysis [17]. The phytochemicals analyzed were alkaloids, flavonoids, tannins, phlobatanins, triterpenes, steroids, saponins and cardiac glycosides.

3. Results and discussion

3.1. Standardization

3.1.1. Effect of boiling time

In order to evaluate the effect of boiling time for the leaf extract preparation, the leaves were boiled for 5, 10 and 15 min. The UV–Vis spectrum of silver nanoparticles was recorded at different time interval of reaction medium. There was very little difference in the formation of AgNPs by 5 and 10 min boiling time but 15 min boiling time decreased the formation of AgNPs (Fig. 1a). Hence, 5 min boiling time was finalized for the preparation of the leaf extract.

3.1.2. Effect of extract amount

In order to evaluate the effect of amount of leaf extract to be added to silver nitrate solution for the formation of AgNPs, different aliquots of 5 min boiled leaf extract (1.5, 3, 4.5 and 6 ml) were added to 40 ml 1 mM $AgNO_3$. The UV–Vis spectrum of AgNPs was recorded at different time interval of reaction medium. The particles synthesis occurred faster in 6 ml extract amount than 1.5, 3, 4.5 ml extract amount (Fig. 1b). SPR intensity was increased with increasing extract amount due to formation of more AgNPs. Hence, 6 ml extract was finalized for the synthesis of AgNPs.

3.2. Characterization

3.2.1. UV–Vis spectral analysis

The leaf extract was light green in color and when it was added to colorless sliver nitrate solution, the solution turned brown rapidly within 10 min; it turned to dark brown and by 2 h the solution turned black (Fig. 1c). The color change occurs due to surface plasmon resonance of silver nanoparticles formed. Intensity of brown color increased in direct proportion to the incubation period and finally it turned black. The characteristic brown color of silver solutions provided a convenient spectroscopic signature to indicate the formation of AgNPs. It was incubated in dark for 24 h at room temperature. The formation of AgNPs occurs from few minutes to hours as reported for different plant extracts [14,18].

The formation of the AgNPs was monitored by UV–Vis spectroscopic analysis. The UV–Vis spectrum of silver nanoparticles recorded at different time interval of reaction medium (0, 10, 20, 30 min) is given in Fig. 1d. The spectrum showed maximum absorption peak at 473 nm (Fig. 1d). The peak observed for synthesized AgNPs was comparable with that of *Iresine herbstii* [19]. The silver was reduced to silver nanoparticles with the help of phytoconstituents such as flavonoids, tannins and triterpenes present in *C. roxburghii* leaf (Table 1). The flavonoids present in the leaf extract are powerful reducing agents which may be suggestive for the formation of AgNPs by reduction of silver nitrate.

3.2.2. FTIR analysis

FTIR analysis was done to identify the possible bio-reducing biomolecules in the extract. The spectra of AgNPs revealed strong bands at 3745.88, 3643.65, 1695.49, 1554.68, 1502.60, 1454.38, 638.46, 613.38, 592.17, 462.93 and 432.70, respectively (Fig. 2). The intense bands at 3745.88, 3643.65 cm^{-1} are characteristic group of O—H stretching of (free) primary alcohols. The peak 1695.49 cm^{-1} corresponds to C═N. The 1554.68 cm^{-1} was identified as the carboxylates (salts) or amino acid zwittorion. The peak of 1502.60 cm^{-1} corresponds to N—O asymmetric stretch of nitro compound. The peak of 1454.38 cm^{-1} corresponds to C—H bend of alkanes. The peak

Table 1 Phytochemical tests of *Cassia roxburghii* leaf powder.

Test	Result
Flavonoids	+ + + +
Tannins	+ + +
Phlobatanins	–
Triterpenes	+ + +
Steroids	–
Saponins	–
Cardiac glycoside	–
Meyer's	+ +
Dragondroff's	+ + +
Wagner's	–
Legal's	–

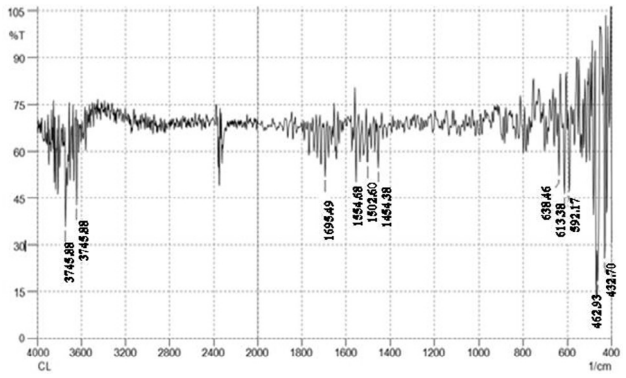

Fig. 2 FTIR spectrum of biosynthesized AgNPs.

of 638.46 cm^{-1} corresponds to C_1C triple bond stretch of alkynes. The peaks of 613.38 and 592.17 cm^{-1} are assigned to the stretching of C—Br and C—I, respectively of alkyl halide group. The peaks of 462.93 and 432.70 cm^{-1} correspond to pyrimidine ring out of plane ring bending (heterocyclic ring). The data indicated the involvement of alcohols, carboxylates, amines, alkanes, alkynes and amino acid residues present in *C. roxburghii* leaf extract in the synthesis of AgNPs.

According to Gole et al. [20] free amino groups or cysteine residues in the proteins can bind to AgNPs and lead to the stabilization of AgNPs by the surface bound proteins. Similar results are reported by Padalia et al. [15]. The FTIR results of the present work suggest that the carbonyl group from the amino acid residues and proteins has stronger ability to bind metal, indicating that the proteins could possibly be involved in capping of silver nanoparticles and thus prevent agglomeration and thereby stabilize the medium. This suggests that the biological molecules could possibly perform dual functions of formation and stabilization of silver nanoparticles in the aqueous medium.

3.2.3. Zeta potential measurement

Zeta potential is an essential parameter for the characterization of stability in aqueous nano suspensions. A minimum of ±30 mV zeta potential values is required for stable nano suspension. The zeta potential of synthesized AgNPs was 34.31 mV. Hence, it can be concluded that the synthesized nanoparticles are fairly stable. It has been stated that secondary metabolites present in the plant are responsible for stabilizing the synthesized nanoparticles. Flavonoids, tannins and terpenoids present in the leaf may be the surface active molecules stabilizing the nanoparticles (Table 1).

3.2.4. XRD analysis

X-ray diffraction (XRD) patterns of silver nanoparticles synthesized using aqueous extract of *C. roxburghii* leaf at room temperature indicate that the structure of silver nanoparticles is face-centered cubic (fcc) (Fig. 3). XRD analysis showed three distinct diffraction peaks at 2 theta values of 15.49°, 15.80° and 15.80° indexed to the (1 1 1), (2 0 0) and (2 2 0) crystalline planes of the fcc structure of metallic silver (lattice Constant a = 4.086 Å, was matched well with Joint Committee on Powder Diffraction Standards (JCPDS) values) (Fig. 3). The sharping of the peak clearly indicated the crystalline nature of the synthesized AgNPs [21].

3.2.5. TEM analysis

The morphology and size of the synthesized particles were determined by Transmission Electron Microscopy (TEM). TEM analysis revealed that the synthesized silver nanoparticles were spherical in shape with average size of the particles ranging from 15 to 20 nm (Fig. 4a–c). Husseiny et al. [22] reported average size of 5–13 nm for AgNPs. Crystalline nature of the green synthesized AgNPs was further confirmed by selected area electron diffraction (SAED) (Fig. 4d). Energy-dispersive X-ray (EDX) spectroscopy analysis was performed to confirm the presence of elemental silver (Fig. 4e). Peaks for Cu and C are from the TEM grid used, and the

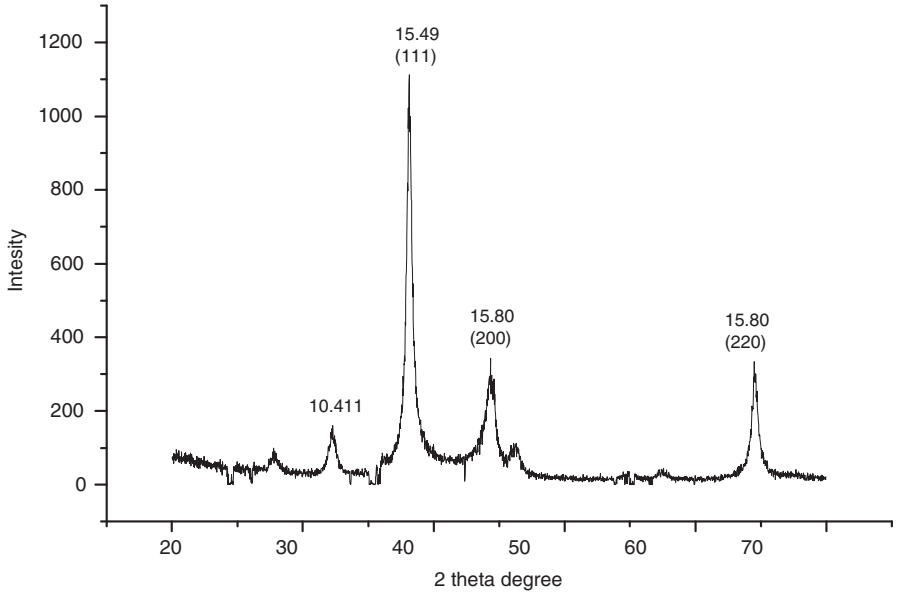

Fig. 3 XRD spectrum of biosynthesized AgNPs.

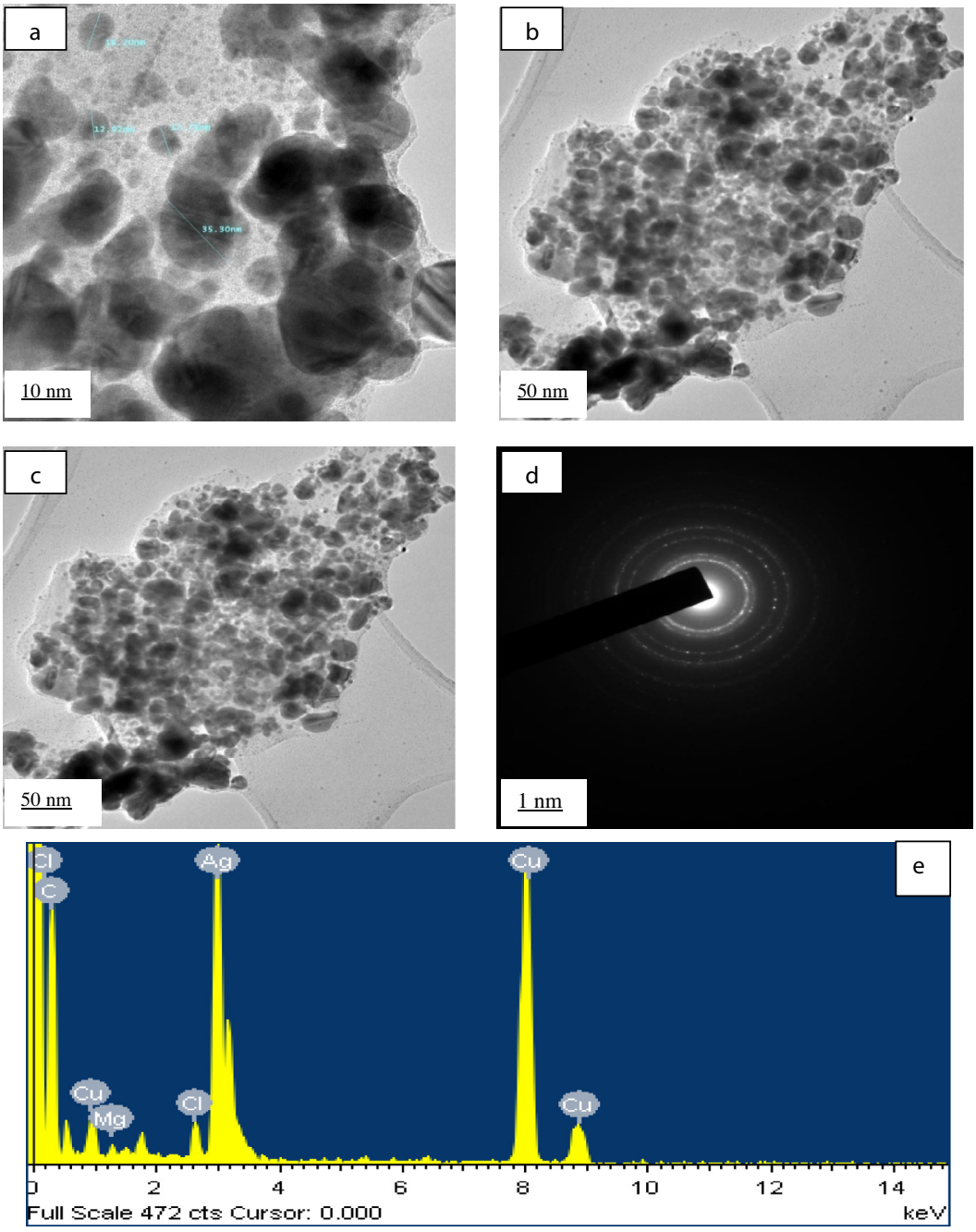

Fig. 4 TEM images (a–c) of Ag nanoparticles in low and high magnification, (d) SAED patterns of the silver nanoparticles and (e) EDX spectrum.

peaks for Mg correspond to the elements of the stabilizing agent present on the surface of AgNPs. Similar results are also reported by Ahamed et al. [23].

3.2.6. Synergistic antimicrobial activity

Antibiotics are generally used to treat many bacterial and fungal infections. But use and misuse of the antibiotics has led for antibiotic resistant microorganisms; there is a steady rise and calls for an urgent alternative source to treat them. In the present work, 15 commercial antibiotics were tested alone and with AgNPs i.e. antibiotics plus AgNPs against two Gram-positive bacteria (*Bacillus cereus* and *Staphylococcus aureus*), two Gram-negative bacteria (*Escherichia coli* and *Pseudomonas aeruginosa*) and four fungi which included 1 clinical isolate (*Candida albicans*, *Candida glabrata*, *Cryptococcus neoformans* and C44 – a clinical isolate). The diameter of inhibition zone was measured, and increase in fold area was calculated.

AgNPs alone did not show any antimicrobial activity while antibiotics alone and antibiotics plus AgNPs showed antimicrobial activity; however the activity of antibiotics plus AgNPs was better than antibiotics alone in most of the microorganisms tested as evidenced by increase in fold area (Tables 2–5). Out of 11 antibiotics tested, synergistic activity i.e. antibiotics plus AgNPs was found with 6 antibiotics against both

Table 2 Synergistic activity of AgNPs of *Cassia roxburghii* leaves with different standard antibiotics against Gram-positive bacteria.

Antibiotic	*B. cereus* (ATCC NO 11778)		Increase in fold area	*S. aureus* (ATCC NO 29737)		Increase in fold area
	Antibiotic(A)	Antibiotic + AgNPs(B)		Antibiotic(A)	Antibiotic + AgNPs(B)	
AMP	–	–	–	33 ± 1	33 ± 0	0
PB^{100}	11 ± 0	11.5 ± 0.5	0.09	9 ± 0	9 ± 0	0
Gen^{10}	19.5 ± 0.5	20.5 ± 0.5	0.10	16 ± 0	16 ± 0	0
C^{30}	33 ± 1	33 ± 1	0	24 ± 4	27 ± 1	0.26
P^{10}	–	–	–	33 ± 3	35 ± 0	0.12
Ak^{10}	22 ± 2	22 ± 1	0	17 ± 0	18 ± 0	0.12
TE^{30}	27.5 ± 0.5	31 ± 1	0.27	28 ± 0	28 ± 0	0
CEP^{30}	13 ± 1	16 ± 2	0.51	37 ± 0.5	37 ± 0	0
AMC^{10}	–	9 ± 0.5		31.5 ± 0.5	32 ± 0	0.03
CFP^{30}	13.5 ± 0.5	14 ± 0	0.07	24 ± 0	27 ± 3	0.26
CC^{10}	14 ± 0	16.5 ± 0.5	0.38	11.5 ± 0	14 ± 0	0.48

AMP – Ampicillin, PB^{100} – Polymyxin, Gen^{10} – Gentamicin, C^{30} – Chloramphenicol, P^{10} – Penicillin-G, AK^{10}– Amikacin, TE^{30} – Tetracycline, CEP^{30} – Cephalothin, AMC^{10} – Amoxyclav, CFP^{30} – Cefpirome, CC^{10} – Clotrimazole.
Mean surface area of the inhibition zone was calculated for each from the mean diameter. Increase in fold area was calculated as $(B^2 - A^2)/A^2$, where A and B are the inhibition zones for antibiotics and antibiotics + Ag-NPs, respectively.

Table 3 Synergistic activity of AgNPs of *Cassia roxburghii* leaves with different standard antibiotics against Gram-negative bacteria.

Antibiotic	*E. coli* (NCIM NO 2931)		Increase in fold area	*P. aeruginosa* (ATCC NO 27853)		Increase in fold area
	Antibiotic(A)	Antibiotic + AgNPs(B)		Antibiotic(A)	Antibiotic + AgNPs(B)	
AMP	9 ± 0	9 ± 0	0	23 ± 1	25 ± 0	0.18
PB^{100}	9 ± 0	9 ± 0	0	13.5 ± 0.5	14.5 ± 0.5	0.15
Gen^{10}	13.5 ± 1.5	16.5 ± 0.5	0.49	22 ± 1	25.5 ± 0.5	0.34
C^{30}	25.5 ± 2.5	27.5 ± 0.5	0.16	14 ± 1	14.5 ± 2.5	0.07
P^{10}	–	–	–	14 ± 0	16 ± 0	0.30
Ak^{10}	17.5 ± 0.5	17.5 ± 0.5	0	24.5 ± 0.5	28 ± 0	0.30
TE^{30}	22 ± 1	27 ± 1	0.50	26.5 ± 0.5	34 ± 1	0.64
CEP^{30}	10 ± 1.5	10 ± 0	0	11 ± 0	11 ± 0	0
AMC^{10}	9 ± 0	9 ± 0	0	20.5 ± 0.5	25 ± 1	0.48
CFP^{30}	9 ± 0	9.5 ± 0.5	0.11	34 ± 1	39 ± 0	0.31
CC^{10}	12 ± 0±	17.5 ± 0.5	1.1	–	–	–

AMP – Ampicillin, PB^{100} – Polymyxin, Gen^{10} – Gentamicin, C^{30} – Chloramphenicol, P^{10} – Penicillin-G, AK^{10}– Amikacin, TE^{30} – Tetracycline, CEP^{30} – Cephalothin, AMC^{10} – Amoxyclav, CFP^{30} – Cefpirome, CC^{10} – Clotrimazole.
Mean surface area of the inhibition zone was calculated for each from the mean diameter. Increase in fold area was calculated as $(B^2 - A^2)/A^2$, where A and B are the inhibition zones for antibiotics and antibiotics + Ag-NPs, respectively.

Table 4 Synergistic activity of AgNPs of *Cassia roxburghii* leaves with different standard antibiotics against fungi.

Antibiotic	*C. glabrata* (NCIM NO 3448)		Increase in fold area	*C. neoformans* (NCIM NO 3542)		Increase in fold area
	Antibiotic (A)	Antibiotic + AgNPs (B)		Antibiotic (A)	Antibiotic + AgNPs (B)	
NS^{100}	29 ± 1	32 ± 0	0.21	23.5 ± 1.5	24.5 ± 0.5	0.08
KT^{30}	24.5 ± 0.5	25 ± 0	0.04	15.5 ± 0.5	17 ± 0	0.20
FLC^{10}	21.5 ± 1.5	24 ± 1	0.24	13.5 ± 1.5	16.5 ± 0.5	0.49
AP^{100}	15 ± 0	16.5 ± 0.5	0.21	12 ± 0	12 ± 0	0

NS^{100} – Nystatin, KT^{30} – Ketoconazole, FLC^{10} – Fluconazole, AP^{100} – Amphotericin B.
Mean surface area of the inhibition zone was calculated for each from the mean diameter. Increase in fold area was calculated as $(B^2 - A^2)/A^2$, where A and B are the inhibition zones for antibiotics and antibiotics + Ag-NPs, respectively.

Gram-positive bacteria *B. cereus* and *S. aureus* as evidenced by increase in the fold area. Maximum increase in fold area was 0.51 and 0.48 against CEP^{30} and CC^{10} (Table 2). The synergistic antibacterial activity against *E. coli* and *P. aeruginosa* was definitely better than that against Gram-positive bacteria. *E. coli* was inhibited by 5 antibiotics and *P. aeruginosa* by 9 antibiotics when antibiotics plus AgNPs were used. Maximum increase in fold area was against CC^{10} (1.1) by *E. coli* while it

Table 5 Synergistic activity of AgNPs of *Cassia roxburghii* leaves with different standard antibiotics against *C. albicans* and clinical isolate (44).

Antifungal	*C. albicans* (NCIM NO 3102)		Increase in fold area	Clinical isolate (44)		Increase in fold area
	Antibiotic (A)	Antibiotic + AgNPs (B)		Antibiotic (A)	Antifungal + AgNPs (B)	
NS^{100}	17 ± 0	17 ± 0	0	21 ± 0	23.5 ± 1.5	0.19
KT^{30}	15 ± 0	18 ± 0	0.44	–	–	–
FLC^{10}	20.5 ± 0.5	20.5 ± 0.5	0	–	–	–
AP^{100}	10.5 ± 0.5	10.5 ± 0.5	0	12 ± 0	14.5 ± 0.5	0.46

NS^{100} – Nystatin, KT^{30} – Ketoconazole, FLC^{10} – Fluconazole, AP^{100} – Amphotericin B.
Mean surface area of the inhibition zone was calculated for each from the mean diameter. Increase in fold area was calculated as $(B^2 - A^2)/A^2$, where A and B are the inhibition zones for antibiotics and antibiotics + Ag-NPs, respectively.

was 0.64 against TE^{30} by *P. aeruginosa* (Table 3). The Gram-positive bacteria are composed of thick peptidoglycan layer while Gram-negative bacteria have thin peptidoglycan layer which facilitates easier penetration of AgNPs into cell wall of Gram-negative bacteria [24]. Jeeva et al. [25] reported moderate antibacterial activity of *C. coriaria* AgNPs against pathogenic bacteria while Fayaz et al. [26] reported enhanced antibacterial activity with antibiotics. Mahitha et al. [27] and Kushwaha and Malik [28] reported antibacterial and antifungal activity of *Bacopa monniera* whole plant and *Verbesina enceliodes* leaf AgNPs respectively. Antibacterial and antifungal activities of AgNPs from *Tephrosia purpurea* leaf extract were reported by Ajitha et al. [29]. The difference in the response with different researchers may be because of the difference in the size and shape of synthesized AgNPs.

The antifungal activity was done with 4 antibiotics against 4 fungal strains; antibiotics plus AgNPs showed activity with all the 4 antibiotics against *C. glabrata* and *C. neoformans* (Table 4) while only KT^{30} plus AgNPs showed activity against *C. albicans* and NS^{100} and AP^{100} showed activity against clinical isolate C44 (Table 5). Maximum activity as evidenced by maximum increase in fold area was against *C. neoformans* by FLC^{10} followed by *C. albicans* against KT^{30}. Kotakadi et al. [30] reported antifungal activity with one antibiotic i.e. fluconazole while Gajbhiye et al. [31] reported antifungal activity with antibiotic amphotericin B. We are perhaps for the first time reporting the combination or synergistic effect of 15 antibiotics with AgNPs against pathogenic bacteria and fungi and it is a new finding. The exact mechanism of antimicrobial activity of AgNPs is not known but it may be because of (i) tyrosine phosphorylation of putative peptides substrates critical for cell viability and cell division, (ii) change in membrane permeability, (iii) loss of replication ability of DNA and ATP production, (iv) formation of free radicals, etc. [32].

3.2.7. Antioxidant activity

Antioxidant efficacy of synthesized AgNPs was evaluated using ABTS radical cation scavenging assay and FRAP assay. $ABTS^{\cdot+}$ is a blue chromophore generated from the oxidation of ABTS by potassium persulfate, in the presence of the plant extract, preformed cation radical gets reduced and employs a specific absorbance at 734 nm, a wavelength remote from the visible region and it requires a short reaction time. The ABTS cation radical scavenging activity increased with increase in the concentration of AgNPs. ABTS cation radical scavenging activity was 27–73% at a concentration range of 40–240 μg/ml (Fig. 5). FRAP assay is based on the ability of antioxidants

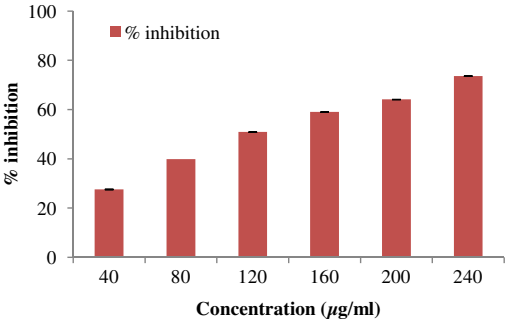

Fig. 5 ABTS radical scavenging activity of AgNPs.

to reduce Fe^{3+} to Fe^{2+} in the presence of TPTZ, forming an intense blue Fe^{2+}-TPTZ complex with an absorption maximum at 593 nm. Ferric reducing antioxidant power (FRAP) of AgNPs was 2.64 (Mg^{-1}). Moteriya and Chanda, [16] reported 23–95% ABTS cation radical scavenging activity and 8.8 Mg^{-1} FRAP activity of AgNPs synthesized using *C. pulcherrima* flower extract.

4. Conclusion

Silver nanoparticles were successfully synthesized using *Cassia roxburghii* leaf extract. The synthesized silver nanoparticles were characterized by UV–Vis spectra, FTIR, XRD and TEM analysis. The maximum absorption peak in UV spectra was 473 nm. X-ray diffraction analysis confirmed the crystalline nature of synthesized AgNPs. TEM analysis revealed the average size to be 15–20 nm. The synthesized AgNPs showed good synergistic antibacterial activity with 15 commercial antibiotics against few pathogenic microorganisms. This is a green, economical and rapid method for the fabrication of AgNPs and they could be utilized as alternative source of antibiotics for the management of multidrug resistant microorganisms. To the best of our knowledge, this is the first report on the biosynthesis, characterization, synergistic antibacterial and antioxidant activity of silver nanoparticles synthesized using *Cassia roxburghii* leaf.

Acknowledgments

The authors thank Department of Biosciences (UGC-CAS) for providing excellent research facilities. Two of the authors Ms. Pooja Moteiya and Hemali Padalia are thankful to UGC, New Delhi for providing Junior Research Fellowship.

References

[1] C. Kamaraj, G. Rajakumar, A.A. Rahuman, K. Velayutham, A. Bagavan, A.A. Zahir, G. Elango, Parasitol. Res. 111 (2012) 2439–2448.

[2] S.W.P. Wijnhoven, W.J.G.M. Peijnenburg, C.A. Herberts, W.I. Hagens, A.G. Oomen, E.H.W. Heugens, B. Roszek, J. Bisschops, I. Gosens, D. Van De Meent, S. Dekkers, W.H. De Jong, M. Van Zijverden, A.J.A.M. Sips, R.E. Geertsma, Nanotoxicology 3 (2009) 109–138.

[3] M.S. Abdel-Aziz, M.S. Shaheen, A.A. El-Nekeety, M.A. Abdel-Wahhab, J. Saudi Chem. Soc. 18 (2014) 356–363.

[4] P. Moteriya, H. Padalia, S. Chanda, J. Pharm. Res. 8 (11) (2014) 1579–1585.

[5] S. Chanda, in: A. Mendez-Vilas (Ed.), Microbial Pathogens and Strategies for Combating Them: Science, Technology and Education, FORMATEX Research Center, Badajoz, Spain, 2013, pp. 1314–1323.

[6] E.K.F. Elbeshehy, A.M. Elazzazy, G. Aggelis, Front. Microbiol. 6 (2015) 453.

[7] I. Willner, R. Baron, B. Willner, J. Adv. Mater. 18 (2006) 1109–1120.

[8] A. Rostami-Vartooni, M. Nasrollahzadeh, M. Alizadeh, J. Colloid Interf. Sci. 470 (2016) 268–275.

[9] N. Muniyappan, N.S. Nagarajan, Process Biochem. 49 (2014) (2014) 1054–1061.

[10] N.J. Reddy, D.N. Vali, M. Rani, S. Sudha, Rani. Mater. Sci. Eng. C 34 (2014) 115–122.

[11] P. Moteriya, S. Chanda, Am. J. Adv. Drug Delivery 2 (4) (2014) 557–575.

[12] N.H. Ali, S.U. Kazmi, S. Faizi, Pak. J. Pharm. Sci. 21 (2008) 21–23.

[13] S. Chanda, M. Kaneria, Y. Baravalia, Afr. J. Biotech. 1 (2012) 2490–2503.

[14] P. Moteriya, S. Chanda, Scientia Iranica 21 (6) (2014) 2499–2507.

[15] H. Padalia, P. Moteriya, S. Chanda, Arab. J. Chem. 8 (2015) 732–741.

[16] P. Moteriya, S. Chanda, Artif. Cells Nanomed. Biotechnol. (2016) (in press). <http://dx.doi.org/10.1080/21691401.2016.1261871>.

[17] J.B. Harborne, Phytochemical Methods, second ed., Chapman & Hall, London, 1973.

[18] S. Bhakya, S. Muthukrishnan, M. Sukumaran, M. Muthukumar, Appl. Nanosci. (2015), http://dx.doi.org/10.1007/s13204-015-0473-z.

[19] C. Dipankar, S. Murugan, Colloids Surf. B: Biointer. 98 (2012) 112–119.

[20] C. Gole, V. Dash, S.R. Ramakrishnaan, A.B. Sainkar, M. Mandal, R.M. Sastry, Langmuir 17 (2001) 1674–1679.

[21] T.Y. Suman, S.R.R. Rajasree, A. Kanchana, S.B. Elizabeth, Colloids Surf. B Biointer. 106 (2013) 74–78.

[22] S.M. Husseiny, T.A. Salah, H.A. Anter, Beni Suef Univ. J. Basic Appl. Sci. 4 (3) (2015) 225–231.

[23] M. Ahamed, M.A.M. Khan, M.K.J. Siddiqui, M.S. Alsalhi, S. A. Alrokayan, Physica E 43 (2011) 1266–1271.

[24] S. Ahmed, M. Ahmad, B.L. Swami, S. Ikram, J. Adv. Res. (2015), http://dx.doi.org/10.1016/j.jare.2015.02.007.

[25] K. Jeeva, M. Thiyagarajan, V. Elangovan, N. Geetha, P. Venkatachalam, Ind. Crops Prod. 52 (2014) 714–720.

[26] A.M. Fayaz, K. Balaji, M. Girilal, R. Yadav, P.T. Kalaichelvan, R. Venkatesan, Nano NBM 6 (2010) 103–109.

[27] B.B. Mahitha, R.B. Deva Prasad, G.R. Dillip, C.M. Reddy, K. Mallikarjuna, L. Manoj, S. Priyanka, K.J. Rao, N.J. Sushma, Dig. J. Nanomater. Biostruct. 6 (2011) 135–142.

[28] H.B. Kushwaha, P. Malik, Turk. J. Biol. 3 (2013) 645–654.

[29] B. Ajitha, Y.A.K. Reddy, P.S. Reddy, Spectrochim. Acta Part A Mol. Biomol. Spectroscosc. 121 (2014) 164–172.

[30] V.S. Kotakadi, S.A. Gaddam, Y. Rao, T.N.V.K.V. Prasad, A. V. Reddy, D.V.R. Sai Gopal, Eur. J. Med. Chem. 73 (2014) 135–140.

[31] M. Gajbhiye, J. Kesharwani, A. Ingle, A. Gade, M. Rai, Nanomed. NBM 5 (2009) 382–386.

[32] C.N. Lok, C.M. Ho, R. Chen, Q.Y. He, W.Y. Yu, H. Sun, P.K. Tam, J.F. Chiu, C.M. Che, J. Proteom. Res. 5 (2006) 916–924.